Retinaldehyde dehydrogenase 2 and Hoxc8 are required in the murine brachial spinal cord for the specification of Lim1+ motoneurons and the correct distribution of Islet1+ motoneurons

Julien Vermot[1], Brigitte Schuhbaur[1], Hervé Le Mouellic[2], Peter McCaffery[3], Jean-Marie Garnier[1], Didier Hentsch[1], Philippe Brûlet[2], Karen Niederreither[4], Pierre Chambon[1], Pascal Dollé[1,*] and Isabelle Le Roux[1,*]

[1]Institut de Génétique et de Biologie Moléculaire et Cellulaire, CNRS/INSERM/Université Louis Pasteur, BP 10142, 67404 Illkirch Cedex, C.U. de Strasbourg, France
[2]Unité d'Embryologie Moléculaire, Institut Pasteur, Bat. J. Monod, 25 rue du Dr Roux, 75724 Paris Cedex 15, France
[3]E. Kennedy Shriver Center, University of Massachusetts Medical School, University of Massachusetts, Waltham, MA 02452, USA
[4]Departments of Medicine and Molecular and Cellular Biology, Center for Cardiovascular Development, Baylor College of Medicine, One Baylor Plaza, Houston, TX 77030, USA
*Authors for correspondence (e-mail: isalr@igbmc.u-strasbg.fr and dolle@igbmc.u-strasbg.fr)

Accepted 5 January 2005

Development 132, 1611-1621
Published by The Company of Biologists 2005
doi:10.1242/dev.01718

Summary

Retinoic acid (RA) activity plays sequential roles during the development of the ventral spinal cord. Here, we have investigated the functions of local RA synthesis in the process of motoneuron specification and early differentiation using a conditional knockout strategy that ablates the function of the retinaldehyde dehydrogenase 2 (Raldh2) synthesizing enzyme essentially in brachial motoneurons, and later in mesenchymal cells at the base of the forelimb. Mutant (*Raldh2*$^{L-/-}$) embryos display an early embryonic loss of a subset of Lim1+ brachial motoneurons, a mispositioning of Islet1+ neurons and inappropriate axonal projections of one of the nerves innervating extensor limb muscles, which lead to an adult forepaw neuromuscular defect. The molecular basis of the *Raldh2*$^{L-/-}$ phenotype relies in part on the deregulation of *Hoxc8,* which in turn regulates the RA receptor RARβ. We further show that *Hoxc8* mutant mice, which exhibit a similar congenital forepaw defect, display at embryonic stages molecular defects that phenocopy the *Raldh2*$^{L-/-}$ motoneuron abnormalities. Thus, interdependent RA signaling and Hox gene functions are required for the specification of brachial motoneurons in the mouse.

Key words: Motoneurons, Retinoic acid, Spinal cord, Raldh2, Hox genes, Lim1, Islet1, Mouse

Introduction

During spinal neurogenesis, neural progenitors acquire positional identity along the anteroposterior (AP) and dorsoventral (DV) axes in response to the spatially restricted action of three main extrinsic signaling pathways: the Shh, Fgf and retinoic acid (RA) pathways (Liu et al., 2001; Mathis et al., 2001; Diez del Corral et al., 2003; Novitch et al., 2003). These pathways control the formation of distinct progenitor domains along the AP and the DV axis, by regulating specific combinations of transcription factors (Appel and Eisen, 2003). Spinal motoneurons originate from a common ventral progenitor domain and acquire columnar subtype identities as revealed by the settling position of their soma and their axonal projections in the periphery (Tosney et al., 1995; Landmesser, 2001). Motoneurons that innervate axial muscles are located in the medial motor columns (MMC) at all AP segmental levels. By contrast, motoneurons that innervate limb muscles are located in the lateral motor columns (LMC) only at brachial and lumbar levels (Tsuchida et al., 1994; Sharma et al., 1998). Two major motoneuron subtypes are generated within the LMC: the medially positioned LMC neurons that innervate the ventral limb muscles and the laterally positioned LMC neurons that innervate the dorsal limb muscles. Motoneurons are subsequently clustered into motor pools, wherein all neurons project to individual muscle targets in the limb (Tosney et al., 1995). The establishment of topographic neural maps requires the coordinated action of factors that: (1) specify motoneuron subtypes; (2) regulate lateral migration and segregation of newly postmitotic neurons to their final settling position; and (3) control axonal guidance to the target muscles. Although various classes of factors, including members of the LIM and Hox homeoprotein families, of the type II cadherin adhesion protein family, of the Ets-related transcription factors and of the Eph/ephrin ligand-receptor tyrosine kinase family (Sharma et al., 1998; Helmbacher et al., 2000; Kania et al., 2000; Livet et al., 2002; Price et al., 2002; Coonan et al., 2003; Dasen et al., 2003; Thaler et al., 2004), have been implicated in the control of these processes, it remains unclear how the action of these factors are coordinated and regulated in postmitotic motoneurons.

In addition to its function during early spinal neurogenesis (Appel and Eisen, 2003), RA signaling plays a major role in

the specification of chicken motoneuron subtypes, soon after these cells withdraw from the cell cycle (Sockanathan and Jessell, 1998; Sockanathan et al., 2003). These sequential roles highlight the importance of the spatiotemporal control of local RA levels, which mainly results from regulated expression of synthesizing enzymes, the retinaldehyde dehydrogenases (Raldh), and metabolizing enzymes, the cytochrome P450s Cyp26 (Niederreither et al., 1999; Abu-Abed et al., 2001; Sakai et al., 2001). Raldh2 acts as the main RA-synthesizing enzyme during early embryogenesis (Niederreither et al., 1999). This enzyme is first expressed in the mesoderm adjacent to the node during early gastrulation; its expression expands to paraxial mesoderm during the phase of early neuronal specification, and at later stages Raldh2 is expressed in LMC neurons (Zhao et al., 1996; Niederreither et al., 1997; Sockanathan and Jessell, 1998; Diez del Corral et al., 2003). In agreement with this expression pattern, transgenic mice that serve as in-vivo reporters of RA signaling have revealed RA activity in early paraxial mesoderm and later in postmitotic cells of the ventral spinal cord at brachial and lumbar levels (Rossant et al., 1991; Colbert et al., 1995; Solomin et al., 1998). As motoneurons exit the cell cycle, they begin to express the homeoprotein Islet1 (Sharma et al., 1998). This expression is rapidly downregulated in lateral LMC neurons when these cells begin to express Lim1, thus generating a molecular distinction between lateral and medial LMC cells (Tsuchida et al., 1994). Lim1 participates to the regulation of the adhesion molecule Epha4, both proteins being required for the proper establishment of topographic projections (Helmbacher et al., 2000; Kania et al., 2000; Kania and Jessell, 2003). The switch from Islet1+ to Lim1+ cells appears to depend on RA provided by early born LMC neurons, as in-vitro and in-vivo exogenous RA exposure of chicken LMC neurons represses Islet1 and promotes Lim1 expression (Sockanathan and Jessell, 1998).

An additional earlier role has been assigned to RA produced by paraxial mesoderm at limb levels in the specification of brachial versus thoracic motor columns, as a blockade of RA signaling prevented the acquisition of an LMC identity by newly generated chick brachial motoneurons, which instead acquired a thoracic character (Sockanathan et al., 2003). Parallel studies have shown that Hoxc proteins, which are expressed at specific AP levels of the spinal cord in both neural progenitors and postmitotic cells, regulate the expression of molecular markers of either thoracic or brachial columnar fate. In particular, Hoxc6 is required for the expression of *Raldh2* in the brachial LMC (Dasen et al., 2003). Conversely, regulation of Hox genes via RA has been described, although at an earlier stage in neural progenitors (Liu et al., 2001). Thus, there seem to be complex interactions between the regulation of RA signaling and Hox gene expression during spinal neurogenesis. Targeted disruptions of *Hoxa10*, *Hoxc8*, *Hoxd9* and *Hoxd10* led to aberrant patterns of motor axon connectivity in the limbs, suggesting roles for Hox proteins in the determination of motoneuron subtypes (Rijli et al., 1995; Carpenter et al., 1997; Tiret et al., 1998; de la Cruz et al., 1999). However, the cellular basis for these defects remains unknown. Retrograde labelings performed on $Hoxc8^{-/-}$ mice revealed a reverse mediolateral position of a subset of motoneurons with respect to their target muscles, suggesting that Hoxc8 is required for establishing the distinction between medial and lateral LMC (Tiret et al., 1998).

To investigate the role of local RA synthesis during the specification of LMC neurons, we have generated mice bearing a conditional mutation that ablates Raldh2 function essentially in developing brachial motoneurons and later in mesenchymal cells at the base of the forelimb. Analysis of these mice indicates that RA synthesis within the LMC plays a crucial role in the brachial LMC in the specification of a subset of lateral cells, in the position of motor cell bodies as well as in the regulation of the expression of transcription factors and adhesion molecules required for correct axonal projections to target muscles. We also report striking similarities in the molecular defects observed in *Raldh2* conditional mutants and *Hoxc8* knockout mice, suggesting that RA signaling and Hox gene functions are essential for the specification of LMC cells.

Materials and methods

Mice

The genomic construct used to generate a conditional (floxed) *Raldh2* allele ($Raldh2^{L2}$) is described elsewhere (Vermot et al., 2003) (J.V. et al., unpublished). *RarbCre* transgenic mice (Moon et al., 2000) were crossed with heterozygous *Raldh2* null mutants (Niederreither et al., 1999) and the resulting $RarbCre\_Raldh2^{+/-}$ mice were bred with $Raldh2^{L2/L2}$ mice to obtain $RarbCre\_Raldh2^{L2/-}$ mutants (hereafter called $Raldh2^{L-/-}$). Littermate animals without the *RarbCre* transgene were used as controls for all experiments. The *Hoxc8* mutant allele was similar to that described previously (Le Mouellic et al., 1992), except that a GFP-Aequorin reporter (G5A) (Baubet et al., 2000) was inserted in place of the *lacZ* gene.

Immunohistochemistry and in-situ hybridization

In-situ hybridization on cryosections was performed as described (Chotteau-Lelièvre et al., 2004). The *Raldh2* probe used to detect both the wild-type and $Raldh2^{L-}$ alleles hybridized with 75 bp of the fourth exon and the subsequent 3′ coding sequence. Other template plasmids were produced in our laboratory (RARβ) or kindly provided by M. Petkovich (*Cyp26B1*), R. Behringer (*Lim1*), C-C. Hui (*Islet1*), S. Pfaff (*Lhx3*), C. Henderson (*Sema3e* and cadherin 7), D. Wilkinson (*Epha4*), R. Klein (*Ephb2*), M. Capecchi (*Hoxc6* and *Hoxc8*), X. Desbiens (*ER81* and *Pea3*), M. Kmita (*lacZ*) and A. Esquela Kerscher (*Gdnf*).

Vibratome (100 μm) sections were processed for immunochemistry (Scardigli et al., 2003) using rabbit polyclonal anti-Epha4 (kindly provided by P. Charnay) (Becker et al., 1995) and mouse monoclonal anti-neurofilament (2H3; Developmental Studies Hybridoma Bank, DSHB) antibodies. X-Gal staining was performed as described (Scardigli et al., 2003).

Double in-situ hybridization and immunolabeling experiments were performed on predissected spinal cords fixed overnight in 4% paraformaldehyde and processed for in-situ hybridization with digoxigenin-labeled probes (Chotteau-Lelièvre et al., 2004), using an InsituPro (Intavis) robot and Fast Red (Roche) to reveal alkaline phosphatase activity. Subsequent immunofluorescence was performed as described (Scardigli et al., 2003) with mouse monoclonal anti-β-galactosidase (Promega), anti-Hoxc8 (C952-7E, Babco), anti-Islet1/2, anti-Lim1/2 and anti-Lim3 (40.2D6, 4F2, and 67.4E12, DSHB), and rabbit polyclonal anti-Raldh2 (Berggren et al., 1999), anti-β-galactosidase (5 prime-3 prime Inc.) and anti-Islet1 (K5, kindly provided by T. Jessell) (Tsuchida et al., 1994) antibodies. Although the latter antibody has been reported to cross-react with Islet2 (Tsuchida et al., 1994), it recognized only Islet1 in our conditions (1.5% of the K5+ cells were Lim1+ per hemisection, whereas 25% of Islet2+ cells were Lim1+, average of 15 sections from five controls). Alexa 488- Alexa 594- and Cy5-coupled secondary antibodies were

used (Molecular Probes and Jackson ImmunoResearch Laboratories, Inc.). Both the sectioned and whole-mount spinal cords were analyzed using a Leica Sp2MP confocal microscope, except for Fig. 8A-C and Fig. 2C,D which were obtained using a Leica macrofluo and macro confocal (D.H. and J. L. Vonesch, unpublished), respectively. Images of cryosectioned spinal cords represent a single focal plan, whereas those of whole-mounts and vibratome sections were obtained by the projection of an average of 20 stacks of pictures (representing 40 μm in thickness). Analysis of dissected spinal cords was performed on a minimum of five control and *Raldh2*$^{L-/-}$ embryos. Analysis of *Hoxc8* mutants was done on two embryos for each genotype; no variation for any marker was observed among each group. Whole-mount anti-neurofilament staining was performed as described (Maina et al., 1997), and embryos were documented on a Leica M420 macroscope. Comparisons between control and mutant spinal cords were performed in all cases on littermate embryos.

Results

Raldh2 expression in the murine brachial LMC

We first analyzed Raldh2 expression in the developing murine brachial spinal cord, using double immunohistochemistry (IHC) with an anti-Raldh2 antibody (Berggren et al., 1999) and an anti-Islet1/2 antibody, which labels all postmitotic motoneurons (Ericson et al., 1992). At embryonic day (E) 9.5, there were few Islet1/2+ cells in the brachial spinal cord and no expression of Raldh2 was observed in these cells, although Raldh2 was expressed in somites and mesenchymal cells surrounding the neural tube (Fig. 1A; see also Fig. 2E). Raldh2 was first detected in Islet1/2+ cells located laterally within the ventral horns at E10-10.5 (Fig. 1B). By analogy with chick spinal cord development, these neurons are likely to correspond to early born motoneurons (Sockanathan and Jessell, 1998). One day later, the MMC neurons located ventrally did not express Raldh2 (Fig. 1C), whereas the LMC cells did. In-situ hybridization of adjacent transverse sections of E12.5 spinal cords showed that *Raldh2* was expressed in the two cell populations of the LMC, the *Islet1*+ cells and the *Lim1*+ cells (Fig. 1D-F).

Generation of *Raldh2* conditional mutant mice

A conditional *Raldh2* allele (*Raldh2*^{L2}) was obtained (Vermot et al., 2003) (J.V. and I.L.R., unpublished). To generate conditional mutants, we used a *RarbCre* transgenic line, in which the regulatory region of the RA receptor RARβ2 controls Cre expression (Moon et al., 2000). This line drives Cre-mediated excision in the developing spinal cord and the trunk mesoderm as early as E8.5 (Moon et al., 2000) (J.V. and I.L.R., unpublished). Cre-positive *Raldh2*$^{L2/-}$ mice (hereafter called *Raldh2*$^{L-/-}$) were obtained at a Mendelian ratio and had a normal life span, but displayed an abnormal flexure of the forepaw digits, especially of the most anterior (second and third) digits (Fig. 2A,B). Partial syndactyly of the second to fourth forelimb digits was also observed, albeit with a variable expressivity (Fig. 2B, arrowheads). No defect was recorded relating to the digit skeleton or the size and topology of distal limb muscle groups and their insertions, except for a slight hypoplasia of the extensor radialis muscles, which control the extension of anterior digits (data not shown). Thus, the abnormal digit flexure phenotype of *Raldh2*$^{L-/-}$ mutants could not be attributed to a specific skeletal or muscle patterning defect.

We then examined the efficiency of the *RarbCre* transgenic line to excise the *Raldh2*^{L2} allele by monitoring Raldh2 immunoreactivity in mutants. At E9.5, Raldh2 expression was not significantly altered in mutants compared with controls (Fig. 2C,D). However, Raldh2 protein was never observed in the brachial spinal cord of mutants at all subsequent stages (E10.5-15.5); residual protein was still present in scattered meningeal and mesenchymal cells surrounding the spinal cord (Fig. 2E-J; and data not shown). Raldh2 expression at E11.5 was also markedly diminished at the level of the brachial plexus (Fig. 2G,H), a region in which motoneurons make pathfinding decisions (Landmesser, 2001). At the lumbar level, a reduced number of Raldh2+ motoneurons was observed in the E12.5 mutant spinal cord (Fig. 2I,J, insets). This residual RA activity can explain the lack of abnormal hind limb phenotype in *Raldh2*$^{L-/-}$ mutants.

Thus, excision of the *Raldh2*^{L2} allele using the *RarbCre* transgenic line led to a complete absence of Raldh2 protein in brachial motoneurons. The pattern of excision of *Raldh2*^{L2}, especially in the mesoderm, was clearly distinct from the pattern of excision described using the same *RarbCre* transgenic mice in the RNA polymerase II large subunit locus (Moon et al., 2000) or the ROSA26 locus (J.V. and I.L.R., unpublished). Our result supports the finding that *LoxP* recombination is locus-position-dependent (Voojs et al., 2001). In summary, the *Raldh2*$^{L-/-}$ mice constitute a model to study the early requirement for local RA synthesis during the early phase of motoneuron specification, and a default in these developmental decisions could be the cause of the adult phenotype.

Altered patterns of RA signaling in brachial *Raldh2*$^{L-/-}$ spinal cord cells

We first examined the distribution of RA-responsive cells within *Raldh2*$^{L-/-}$ spinal cord using an RA-responsive reporter transgenic line (*RARE_hsp68_lacZ*) (Rossant et al., 1991). The

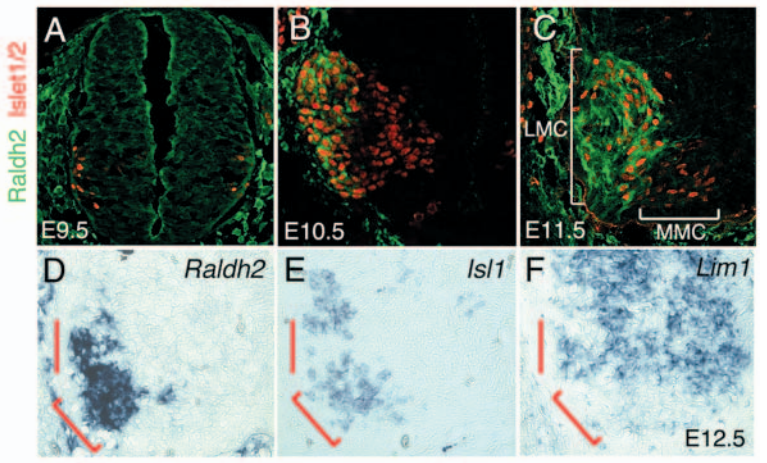

Fig. 1. Expression of Raldh2 in the murine brachial LMC. (A-C) Immunodetection of Raldh2 (green) and Islet1/2 (red) proteins on transverse spinal cord sections. (E-F) *Raldh2*, *Islet1* and *Lim1* transcripts on adjacent transverse spinal cord sections, at the posterior LMC level. The *Islet1* and *Lim1* subpopulations within the LMC are marked by brackets and vertical lines, respectively.

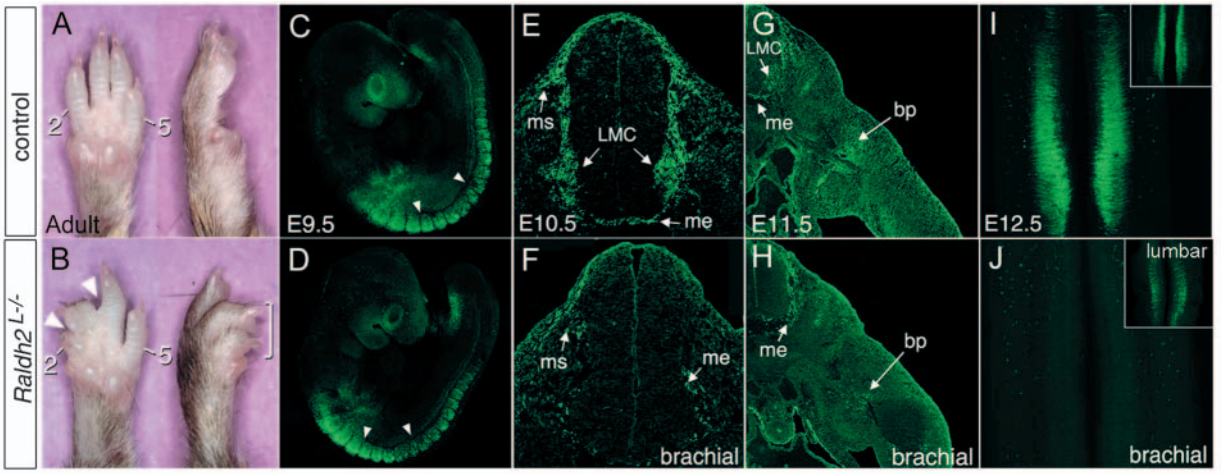

Fig. 2. Adult phenotype and Raldh2 protein analysis in *Raldh2*$^{L-/-}$ mutants. (A,B) Ventral (left) and profile (right) views of the forepaws of 2-month-old mice. Note the abnormal flexure of anterior digits (bracket) and partial fusion between digits 2, 3 and 4 (arrowheads). (C,J) Immunodetection of Raldh2 on whole-mount embryos (C,D), transverse sections at the level of the brachial spinal cord (E-H) and dissected spinal cords flattened into an 'open book' configuration (I,J). Arrowheads (C,D) highlight the brachial region. 2,5, digit numbers; bp, brachial plexus; me, meningeal cells; ms, mesenchymal cells.

patterns of β-galactosidase (β-Gal) expression were analyzed by immunofluorescence in control and *Raldh2*$^{L-/-}$ transgenic embryos. In E10.5 control embryos, β-Gal+ cells were scattered along the DV axis of the brachial spinal cord (Fig. 3A). In *Raldh2*$^{L-/-}$ mutants, fewer β–Gal+ cells were found in the ventral horns and in the dorsalmost region of the brachial spinal cord (Fig. 3B). We further showed that in the E11.5 control ventral spinal cord, some Islet1/2+ cells expressed β-Gal (Fig. 3C, arrows), whereas no Islet1/2+ cells were β-Gal+ in *Raldh2*$^{L-/-}$ spinal cords (Fig. 3D), indicating the depletion of RA-responsive motoneurons. At E12.5, β-Gal+ cells were distributed along the dorsal and intermediate regions of control flat-mounted spinal cords (Fig. 3E). By contrast, in *Raldh2*$^{L-/-}$ mutants, β-Gal+ cells were essentially found in a broad longitudinal band within the intermediate region of the spinal cord (Fig. 3F, brackets). This pattern is reminiscent of RA activity in *Raldh2* null mutants rescued by RA supplementation (Mic et al., 2002; Niederreither et al., 2002).

We then analyzed the expression of *Rarb*, the main RAR expressed during LMC specification (see Colbert et al., 1995), on flat-mounts and serial transverse sections of E12.5 spinal cords (Fig. 3G-L). *Rarb* expression was downregulated within the *Raldh2*$^{L-/-}$ motor columns, particularly at the level of the *Islet1*+ posterior medial domain, which exhibited strongest expression in controls (Fig. 3L, asterisk). These results, in agreement with a previous study which showed that excess RA induces ectopic *Rarb* expression in the spinal cord (Colbert et al., 1995), demonstrate that lack of local RA synthesis in *Raldh2*$^{L-/-}$ spinal cord leads to a decrease of RARβ-mediated activity in specific motor pools.

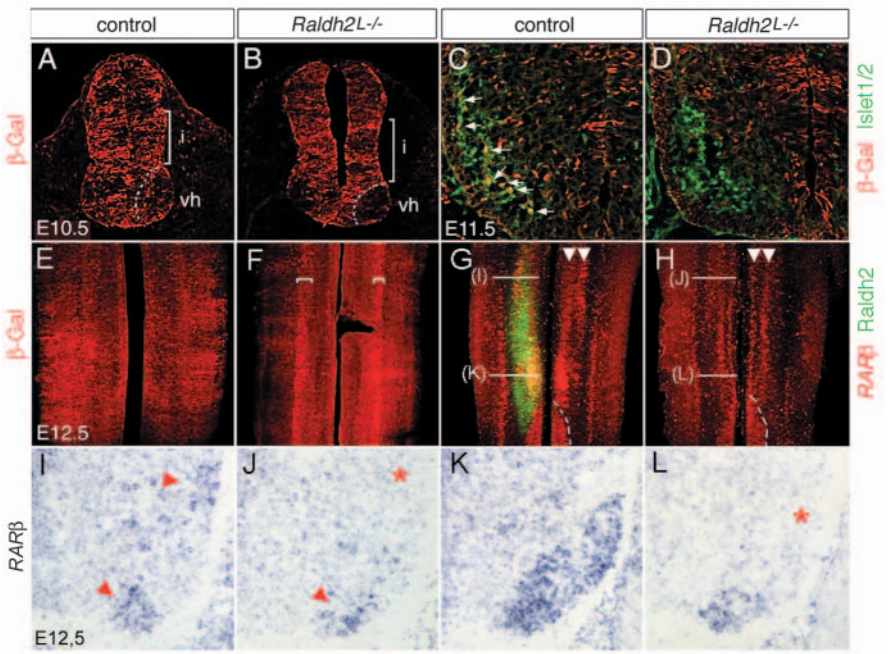

Fig. 3. Altered distribution of RA-responsive cells in *Raldh2*$^{L-/-}$ brachial spinal cord. (A-F) Immunodetection of β-Gal (red) on transverse ventral spinal cord sections (A-D) and dissected spinal cords (E-F) in *RARE_hsp68_lacZ* transgenic mice. (C,D) Combined immunodetection of β-Gal (red) and Islet1/2 (green). Arrows point to β-Gal+/Islet1/2+ cells (orange). Brackets in (F) indicate abnormal β-Gal distribution in a broad longitudinal band within the intermediate region. (G,H) *Rarb* transcript distribution (red) combined to Raldh2 immunofluorescence (green) on flat-mounted spinal cords. (G) Composite image in which the overlay of the two signals is shown on the left side only. The dotted lines in (G,H) point to the thoracic MMC. (I,L) *Rarb* transcripts on transverse ventral spinal cord sections at two different AP levels as indicated in E,F. Arrowheads point to *Rarb*+ motor columns and asterisks show a deficiency of *Rarb*+ cells in mutants compared with controls. i, intermediate region; vh, ventral horns.

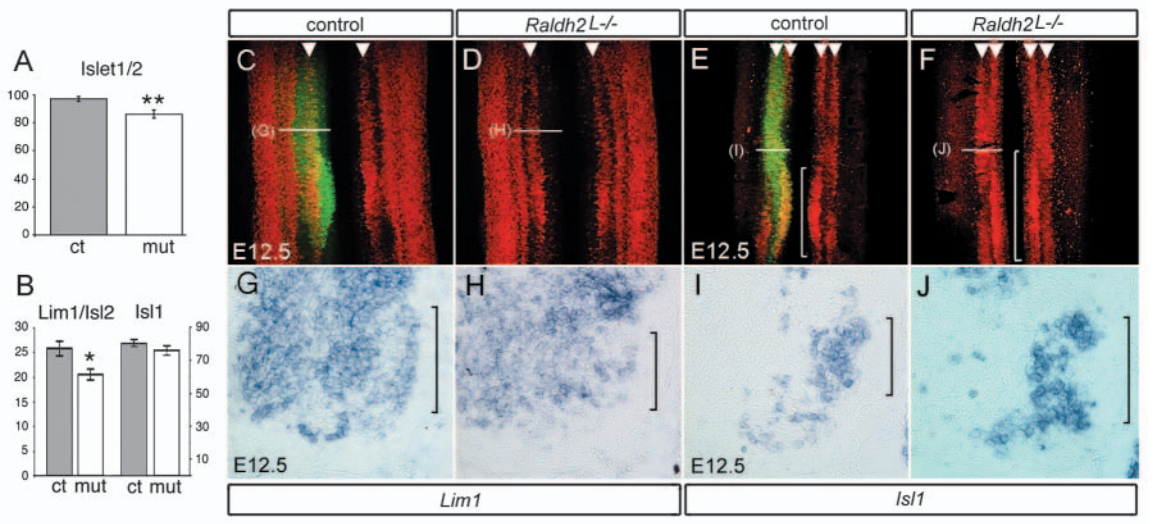

Fig. 4. Abnormal distributions of *Islet1*+ and *Lim1*+ cells in *Raldh2*$^{L-/-}$ brachial spinal cord. (A) Quantitation of Islet1/2+ motoneurons in the brachial LMC of E11.5 control and *Raldh2*$^{L-/-}$ embryos (Y axis: number of motoneurons per hemisection; ct: 96.84±1.77; mut: 86.04±3; mean±s.e.m.; *t*-test: *P*=0.009; ten sections spanning the Raldh2 LMC domain were counted in nine embryos of each genotype). (B) Quantitation of Lim1/2/Islet2+ and Islet1+ motoneurons per hemisection in the brachial LMC of E11.5 control and *Raldh2*$^{L-/-}$ embryos. The number of Lim1/2/Islet2+ cells was significantly decreased in mutants (Lim1/2/Islet2: ct, 25.78±1.48; mut, 20.50±1.11; mean±s.e.m.; *t*-test *P*=0.024; ten sections were counted in five embryos of each genotype), whereas the number of Islet1+ cells was similar in mutants and controls (Islet1: ct, 80.36±2.68, mut, 76.28±2.94; mean±s.e.m.; *t*-test *P*=0.336). (C-F) *Lim1* (C,D, red) and *Islet1* (E,F, red) transcripts on flat-mounted spinal cords combined with Raldh2 immunofluorescence (C,E, green). (C,E) Composite images in which the overlay of the two signals is shown on the left side only. (E,F) The posterior domain of high *Islet1* expression, marked by a bracket, is expanded anteriorly in the mutant. *Lim1*+ and *Islet1*+ motor columns are indicated by arrowheads. (G-I) *Lim1*+ (G,H) and *Islet1*+ (I,J) transcripts on transverse ventral spinal cord sections at levels indicated by horizontal arrows in C-F. The *Islet1* and *Lim1* subpopulations within the LMC are marked by brackets.

Loss of *Lim1*+ cells and redistribution of *Islet1*+ cells in *Raldh2*$^{L-/-}$ spinal cord

We then analyzed the identity of the brachial LMC neurons in *Raldh2*$^{L-/-}$ mutants. We first quantified the number of Islet1/2+ motoneurons in the ventral spinal cord at E11.5. Islet1/2+ cells were counted on serial transverse sections spanning the entire *Raldh2* domain, which was mapped by in-situ hybridization (see Materials and methods). A significant 10% decrease of the number of Islet1/2+ cells was found in mutants (Fig. 4A). Double IHC was performed on adjacent control and mutant sections using: (1) an anti-Lim1/2 antibody; and (2) an anti-Islet2 antibody (Fig. 4B) or an anti-Islet1 antibody (K5 antibody; Fig. 4C; see Materials and methods) to quantify Lim1+ or Islet1+ motoneurons. We found that, within the *Raldh2* domain, the number of Islet1+ cells (medial LMC and MMC cells) was unchanged in *Raldh2*$^{L-/-}$ mutants compared with controls, whereas the number of Lim1+/Islet2+ motoneurons (lateral LMC cells) was significantly decreased by about 20% in mutants (Fig. 4B).

We next looked at the distribution of *Lim1*+ and *Islet1*+ transcripts on E12.5 flattened spinal cords. The downregulation of *Lim1* expression was visible in the motor column in mutants, whereas no change in the interneuron dorsal domain was noticeable (Fig. 4C,D). Surprisingly, the spatial distribution of *Islet1* was altered in mutants (Fig. 4E,F). Two classes of phenotypes were obtained at about the same frequency. In the first class (data not shown; *n*=13), the two *Islet1*+ columns were continuous along the AP axis, instead of being interrupted by *Islet1*– cells. In the second, more severe class (Fig. 4F; *n*=11), *Islet1* was no longer distributed into two columns in the anterior LMC, but instead was uniformly expressed. In all cases, the domain of high *Islet1* expression in the posterior LMC was expanded in mutants (brackets, Fig. 4E,F). We further confirmed the decrease of *Lim1* expression in motoneurons and the change in *Islet1* distribution by in-situ hybridization of adjacent sections at various AP levels of the LMC (Fig. 4G-J, and data not shown).

Alterations of the Lim1+ and Pea3+ motor pools in *Raldh2*$^{L-/-}$ brachial LMC

We next analyzed the expression of selective markers of LMC motor pools. The overall organization of the LMC was not disrupted in *Raldh2*$^{L-/-}$ spinal cord. Indeed, the expression domain of *Ephb2*, which closely matches that of Raldh2 in controls (Fig. 5A), was not spatially altered in mutants (Fig. 5A-D). In addition, the organization of the MMC (*Lim3*+ cells) and V2 columns (*Chx10*+ cells) were not modified in mutants, indicating that no change of the identity of LMC neurons toward MMC neurons or V2 interneurons had occurred in the mutants (data not shown). By contrast, we found a consistent decrease of the expression of cadherin 7 and *Epha4* in the Lim1+ lateral LMC posterior domain, confirming the loss of a subset of Lim1+ cells (data not shown, and Fig. 5E-H).

We also found that cells expressing the Ets-related transcription factor *Pea3* were mispositioned within the LMC in mutants. The *Pea3*+ motor pool is located in the posterior medial LMC and is constituted by over 95% of Islet1+ cells at segmental levels C7/8 (Livet et al., 2002) (Fig. 5I,K). Although the *Pea3* expression domain spanned a comparable length in control and mutant spinal cords at E12.5 (brackets, Fig. 5I,J),

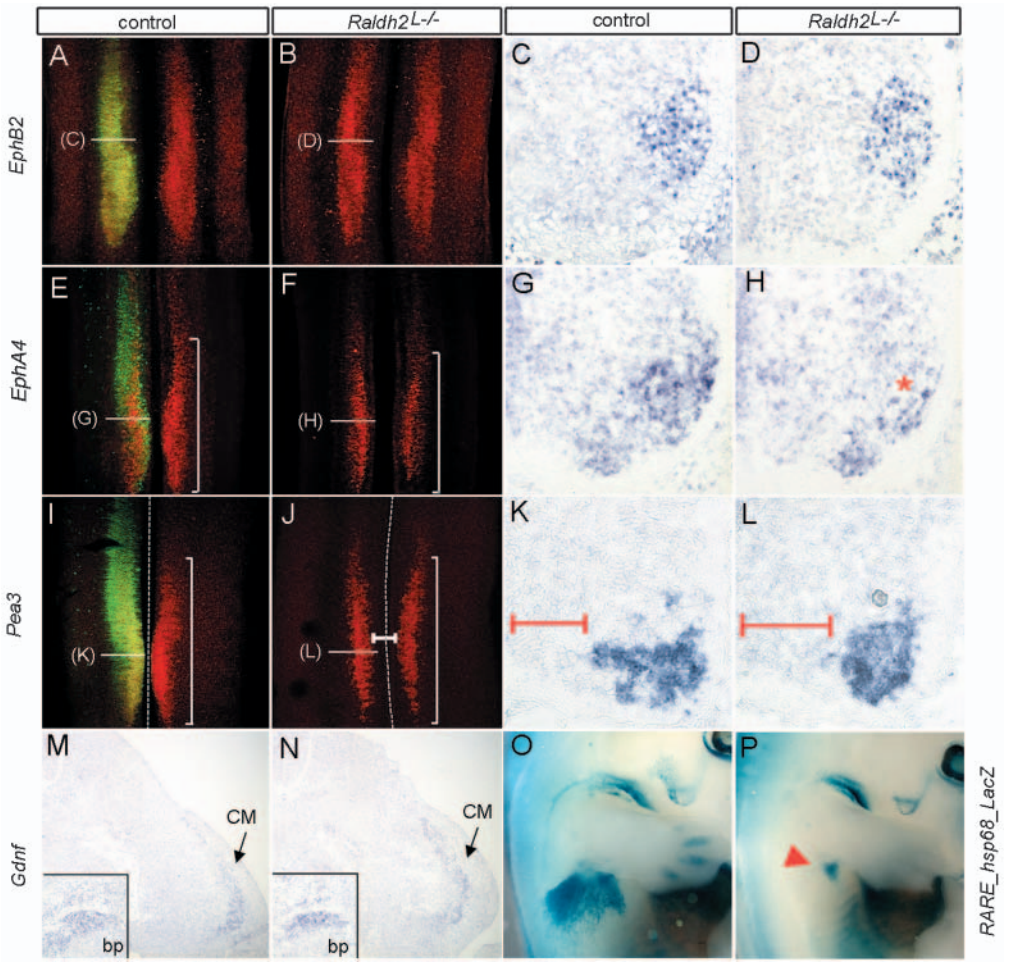

Fig. 5. Alterations of specific motor pools in *Raldh2*$^{L-/-}$ brachial LMC at E12.5. (A-D) *Ephb2* transcripts on flat-mounted spinal cords (A,B) and transverse sections (C,D) at levels indicated in A,B. (E-H) *Epha4* transcripts on flat-mounted spinal cords (E,F) and transverse sections (G,H) at levels indicated in E,F. Brackets (E,F) indicate the extent of the *Epha4* motor pools along the AP axis. The asterisk (H) points to decreased *Epha4* signal in the *Raldh2*$^{L-/-}$ lateral LMC. (I-L) *Pea3* transcripts on flat-mounted spinal cords (I,J) and transverse sections (K,L) at levels indicated in I,J. Horizontal bars (white in J and red in K,L) delineate the larger distance between the ventral midline (dotted lines, I,J) and the *Pea3*+ cells in mutants. Raldh2 immunofluorescence has been combined with in-situ hybridization on control spinal cords (A,E,I, green), the overlay of the two signals is shown on the left side only. (M,N) *Gdnf* transcripts on transverse sections at thoracic and brachial plexus (bp; insets) levels. (O,P) X-gal staining of *RARE_hsp68_lacZ* transgenic embryos. (P) The red arrowhead points to the almost complete absence of staining in the cutaneous maximus (CM) hypaxial muscle.

the distance between the ventral midline and the *Pea3*+ cells was markedly larger in mutants (horizontal bars, Fig. 5L). A similar observation was made with *Semaphorin3E*, which marks a subset of *Pea3*+ cells (data not shown). *Pea3* expression is regulated by glial cell-derived neurotrophic factor (Gdnf) produced at the level of the brachial plexus and later, in the hypaxial muscles innervated by Pea3+ motoneurons, the latissimus dorsi (LD) and cutaneous maximus (CM) (Haase et al., 2002; Livet et al., 2002). We then examined whether *Gdnf* expression was altered in mutants at E12.5. No significant change was detected in the distribution and levels of *Gdnf* transcripts, neither at the level of the brachial plexus nor in the CM in mutants, compared with controls (Fig. 5M,N). As these tissues display endogenous RA activity in control embryos (Fig. 5O), we monitored this activity in mutant embryos using the *RARE_hsp68_lacZ* transgene. A drastic decrease of β-Gal reporter activity was seen at the level of the brachial plexus at E11.5 (data not shown), and one day later in the LD and CM muscles in *Raldh2*$^{L-/-}$ embryos (Fig. 5P). Together, these data suggest that RA activity in the periphery does not regulate the expression of *Gdnf,* and therefore that the decreased RA activity in the periphery is unlikely to be the primary cause of mispositioned Pea3+ cells within the *Raldh2*$^{L-/-}$ LMC.

Impaired dorsal motor axonal projections in *Raldh2*$^{L-/-}$ embryos

In an attempt to establish a link between the LMC molecular defects described above with the adult *Raldh2*$^{L-/-}$ phenotype, we investigated the development of forelimb motor axonal projections. We first analyzed by double IHC at E11.5 the expression of neurofilament and Epha4, the latter being preferentially expressed in axons projecting dorsally in the wild-type limb bud (Helmbacher et al., 2000; Kania and Jessell, 2003). Neurofilament distribution revealed no obvious defect in motor axonal projections in mutants (Fig. 6A,B). By contrast, the expression of Epha4 was significantly diminished in the dorsal axonal projections in *Raldh2*$^{L-/-}$ forelimb (Fig. 6C,D, thin arrows). Epha4 expression in the proximal-dorsal limb mesenchyme was unaffected in mutants (Fig. 6C,D, arrowheads), suggesting that the lack of this protein in dorsal axons is linked to the corresponding motor pool defect (Fig. 5E-H).

Brachial axonal projections were further analyzed at later stages using whole-mount anti-neurofilament IHC. At E12.5, the growing forelimb axonal projections, the arrangement of the developing brachial plexus and its spinal roots were not detectably altered in *Raldh2*$^{L-/-}$ embryos (data not shown). Almost all the growing nerve tracts were normally patterned at E13.5 and 14.5 in mutants (Fig. 6E,F and data not shown). However, the distal projections of the ramus profundus of the radialis nerve supplying most of the extensor muscles of the forepaw were severely atrophied (Fig. 6H, arrowheads and inset). We conclude that the forepaw prehension deficiency of *Raldh2*$^{L-/-}$ mice is likely to result from projection defects of the ramus profundus of the radialis nerve.

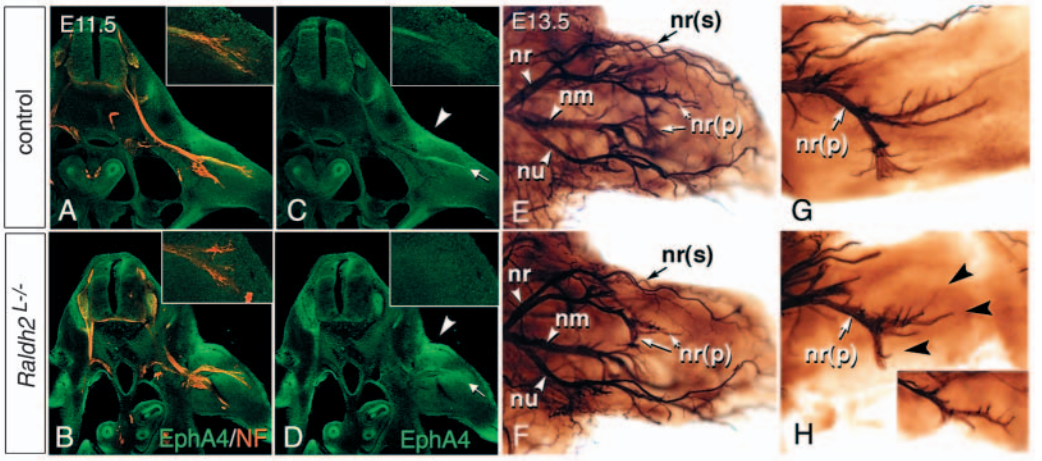

Fig. 6. Impaired development of dorsal forelimb nerve branches in *Raldh2*$^{L-/-}$ embryos. (A-D) Combined immunodetection of Epha4 (green) and neurofilaments (red) on transverse sections of E11.5 embryos. (C,D) Epha4 signal alone. Insets show high magnifications of the extremities of the growing dorsal nerves. EphA4 is greatly diminished in the distal tip of the growing dorsal nerves in mutants (thin arrows). Epha4 level in the dorsal limb mesenchyme is not altered in the mutant (arrowheads). (E-H) Nerve patterns in the developing forelimb, using whole-mount anti-neurofilament IHC. (G,H) Details of the growing axons of the ramus profundus of the radialis nerve, viewed after removal of other nerve branches. The corresponding nerve from another, more severely affected mutant, is shown at the same magnification in an inset. nm, nerve medianus; nr: nerve radialis; nr(p), nr(s), profundus and superficialis ramii of the nerve radialis, respectively; nu, nerve ulnaris.

Downregulation of *Hoxc6* and *Hoxc8* expression in *Raldh2*$^{L-/-}$ LMC

The forelimb defect observed in *Raldh2*$^{L-/-}$ mice is reminiscent of the *Hoxc8* knockout mouse phenotype (Le Mouellic et al., 1992; Tiret et al., 1998). We hypothesized that decreased local RA signaling could affect Hox gene expression in the brachial LMC. *Hoxc6* and *Hoxc8* expression were therefore analyzed at E12.5. While in controls *Hoxc6* was broadly expressed in the Raldh2 domain (Fig. 7A), in *Raldh2*$^{L-/-}$ spinal cord its expression was abnormally low, especially in the central LMC domain (brackets, Fig. 7A,B). In controls, *Hoxc8* was expressed at the anterior level of the LMC in the *Lim1*+ interneuron column, while at the posterior level of the LMC it was additionally expressed in the *Islet1*+ and *Lim1*+ motor columns (Fig. 7C,E). In mutants, the Hoxc8 interneuron domain was comparable to that of controls, whereas the anterior boundary of *Hoxc8* expression in the motoneurons was shifted posteriorly at the transcript and protein levels (Fig. 7C-L). Hoxc8 downregulation was most prominent in the *Lim1*+ motor column, as shown in dissected spinal cords co-labeled with *Lim1* and on serial transverse sections (red arrows, Fig. 7E-L). Taken together, these data show that decreased RA signaling affects Hox gene expression within LMC neurons, which may in turn play a role in the molecular alterations described in the *Raldh2*$^{L-/-}$ LMC.

Loss of Hoxc8 function phenocopies the molecular defects of *Raldh2*$^{L-/-}$ spinal cord

To verify this hypothesis, we performed a molecular analysis of the brachial spinal cord in *Hoxc8* mutant mice (Le Mouellic et al., 1992; Tiret et al., 1998). Raldh2 expression in the LMC was comparable to that of controls in *Hoxc8*$^{+/-}$ mice, whereas its expression domain was thinner in the posterior LMC in *Hoxc8*$^{-/-}$ mutants at E12.5 (Fig. 8A-C). This phenotype was partly due to a loss of Raldh2+ cells in the *Islet1*+ domain (Fig. 8J-L). We next examined the expression of *Rarb*, a known direct RA-target gene (de Thé et al., 1990; Sucov et al., 1990). In the *Hoxc8*$^{+/-}$ LMC, *Rarb* was selectively downregulated in the Islet1+ posterior medial domain (Fig. 8D,E, brackets), whereas its expression was abolished in the *Hoxc8*$^{-/-}$ brachial LMC (Fig. 8F). These data clearly indicate that RA activity is altered in *Hoxc8*$^{+/-}$ and *Hoxc8*$^{-/-}$ spinal cords.

In *Hoxc8*$^{+/-}$ and *Hoxc8*$^{-/-}$ mutants, expression of *Lim1* was downregulated in the posterior LMC (Fig. 8G-I) and *Islet1*+ cells were abnormally distributed (Fig. 8J-L). In *Hoxc8*$^{+/-}$ mice, *Islet1* was continuously distributed in two thick longitudinal columns throughout the LMC (Fig. 8K, arrowheads). In *Hoxc8*$^{-/-}$ mutants, *Islet1*+ cells spanned a uniform domain throughout most of the LMC (Fig. 8L). The analysis of *Islet1* expression on serial transverse sections revealed ectopic dorsal *Islet1*+ cells at the level of the posterior LMC in *Hoxc8*$^{+/-}$ mice, and this abnormality was more pronounced in *Hoxc8*$^{-/-}$ embryos (Fig. 8K,L). Analysis of *Pea3* expression showed a mislocation of these cells in *Hoxc8*$^{+/-}$ mutants: the distance between the ventral midline and the *Pea3*+ cells was larger in mutants (Fig. 8N, horizontal bars). *Pea3* expression was greatly diminished in *Hoxc8*$^{-/-}$ mutants, and the ventral migration of these cells did not occur properly (Fig. 8O). In both *Hoxc8*$^{+/-}$ and *Hoxc8*$^{-/-}$ mutants, the distribution and levels of *Gdnf* transcripts in the brachial plexus and the CM muscle was comparable to those of wild-type embryos (Fig. 8P-R).

Taken together, the analysis of the *Hoxc8* mutant spinal cords revealed striking similarities with the abnormalities found in *Raldh2*$^{L-/-}$ mutant mice, including a decrease in RA activity monitored by the expression of *Rarb*, a downregulation of *Lim1* expression within the motor columns, a redistribution of *Islet1*+ cells and a mispositioning of *Pea3*+ cells. It was found, however, that *Hoxc8*$^{+/-}$ heterozygous mutants most closely phenocopied the *Raldh2*$^{L-/-}$ spinal cord phenotype, whereas *Hoxc8*$^{-/-}$ homozygous mice clearly exhibited more severe cellular defects.

Discussion

This study provides evidence that Raldh2 and Hoxc8 functions within the brachial spinal cord are required for the expression of a subset of Lim1+ motoneurons, the correct positioning of Islet1+ motor cell bodies and their appropriate axonal projections. We discuss these findings in the context of the role

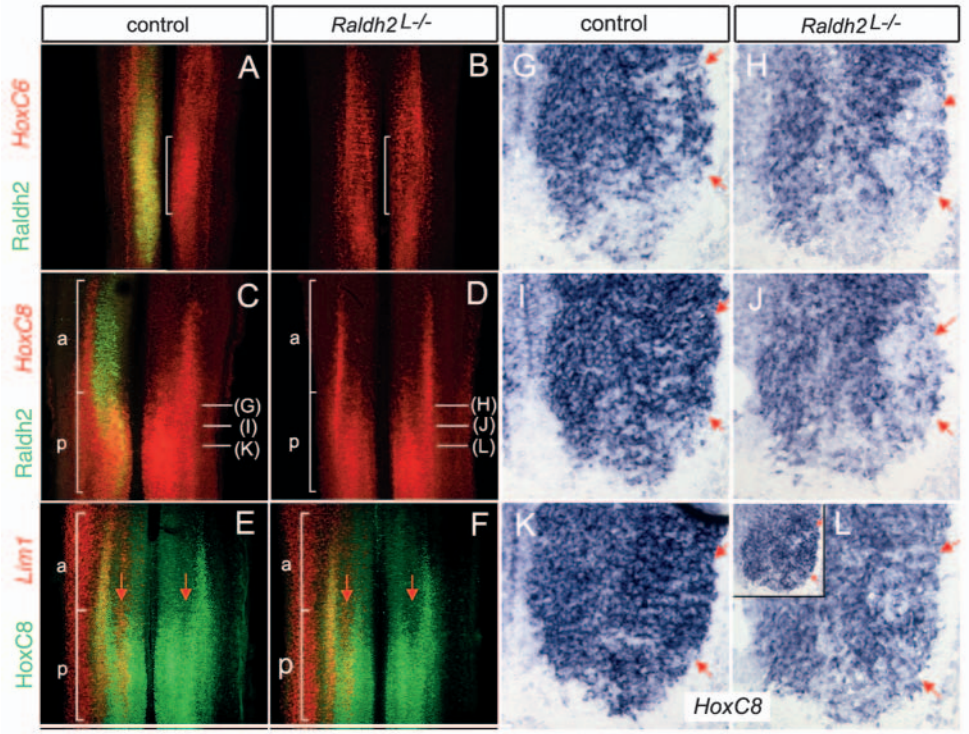

Fig. 7. Decreased expression of *Hoxc6* and *Hoxc8* in *Raldh2*$^{L-/-}$ brachial LMC. (A-D) Combined Raldh2 immunofluorescence (green, left side) and *Hoxc6* (A,B, red) or *Hoxc8* (C,D, red) in-situ hybridization on dissected spinal cords. In *Raldh2*$^{L-/-}$ mutant, *Hoxc6* expression is diminished preferentially within its central domain (A,B, brackets). (E,F) Combined Hoxc8 immunofluorescence (green) and *Lim1* in-situ hybridization (red). A posterior shift of Hoxc8 protein is observed in *Raldh2*$^{L-/-}$ spinal cord, mostly within the *Lim1*+ motor column (red arrows). (G-L) *Hoxc8* transcripts on serial transverse sections at levels indicated in C and D; 70 μm separate each section plane. The inset in L shows the following posterior section in which *Hoxc8* transcript distribution in the mutant is comparable to the previous control section (compare with K). Two red arrows delineate the Lim1+ LMC domain. a, anterior; p, posterior.

of RARβ as a pivotal molecule for the integration of signals during motoneuron specification.

RARβ, a key component of the RA signaling pathway during motoneuron specification

Our findings show that the regulation of RA signaling in the LMC cells depends at least on the activity of two molecules: Raldh2 and RARβ. It is noteworthy that the skeletal analysis of the forepaw of compound RARβ/RARγ mutant mice revealed a retraction of the digits that resembles the *Raldh2*$^{L-/-}$ phenotype (Ghyselinck et al., 1997). Unlike Raldh2, which is uniformly expressed in the LMC cells, *Rarb* expression is dynamic, suggesting that this receptor plays a key role in the spatiotemporal regulation of RA activity during the specification of motoneurons. At E11.5, *Rarb* expression in the spinal cord was similar to that of the *RARE_hsp68_lacZ* reporter transgene, whereas one day later it became restricted to specific motor pools (Fig. 3, and data not shown). These expression patterns most probably reflect the sequential roles of RARβ-mediated RA signaling during motoneuron differentiation.

Local RA synthesis within the spinal cord is required for the specification of a subset of Lim1+ LMC cells

The analysis of *Raldh2*$^{L-/-}$ mutant mice did not reveal any re-specification of the LMC cells toward another cell fate; for example, no re-specification of the LMC cells toward thoracic motoneuron fates such as the MMC cells or preganglionic motoneurons (PrGG) was observed (I.L.R., unpublished). As RA signaling provided by the paraxial mesoderm has been shown to specify a brachial versus thoracic motor column fate (Sockanathan et al., 2003), our data are in agreement with the fact that *RarbCre*-mediated excision of *Raldh2*^{L2} allele mostly occurs within the spinal cord and does not significantly deplete Raldh2 function in paraxial mesoderm during the phase of brachial versus thoracic fate decision.

We observed in *Raldh2*$^{L-/-}$ mutant mice a decrease of 10% in the number of motoneurons at E11.5 (Fig. 4). This decrease is cell type specific, as it only affects the *Lim1*+ population. A decrease in the proliferation of motoneuron progenitors or a premature cell death of postmitotic *Lim1*+ cells could explain this phenomenon. We favor the second hypothesis, because no reduction in RA-responsive cells was observed in ventral neural progenitors at E9.5 and 10.5 in the *Raldh2*$^{L-/-}$ mutants (Fig. 3B). Our results thus confirm previous findings that demonstrated the role of RA signaling in the specification of chick lateral LMC neuronal identity (Sockanathan and Jessell, 1998).

The whole range of later developmental (from E12.5) and postnatal defects observed in *Raldh2*$^{L-/-}$ mice cannot, however, be explained by the early death of a subset of Lim1+ motoneurons, or by an increased rate of the normally occurring programmed cell death, as TUNEL experiments performed at E13.5 did not show significant differences between controls and mutants (I.L.R., unpublished). The abnormal axonal arborization of a branch of the radialis nerve and the decreased Epha4 protein expression in the growing dorsal limb axons indicate sustained functional defects in specific motor pools (Fig. 6). One possibility is that RA deficiency leads to the acquisition of an incomplete motoneuron identity and to the presence of motoneurons that neither expressed *Islet1* nor *Lim1* and, therefore, cannot properly express differentiation markers.

RA synthesis is required for the correct positioning of Islet1+ motoneurons, including Pea3+ cells

We found that *Pea3*+ motoneurons were mispositioned in the *Raldh2*$^{L-/-}$ posterior LMC. Although the expression of *Pea3* in

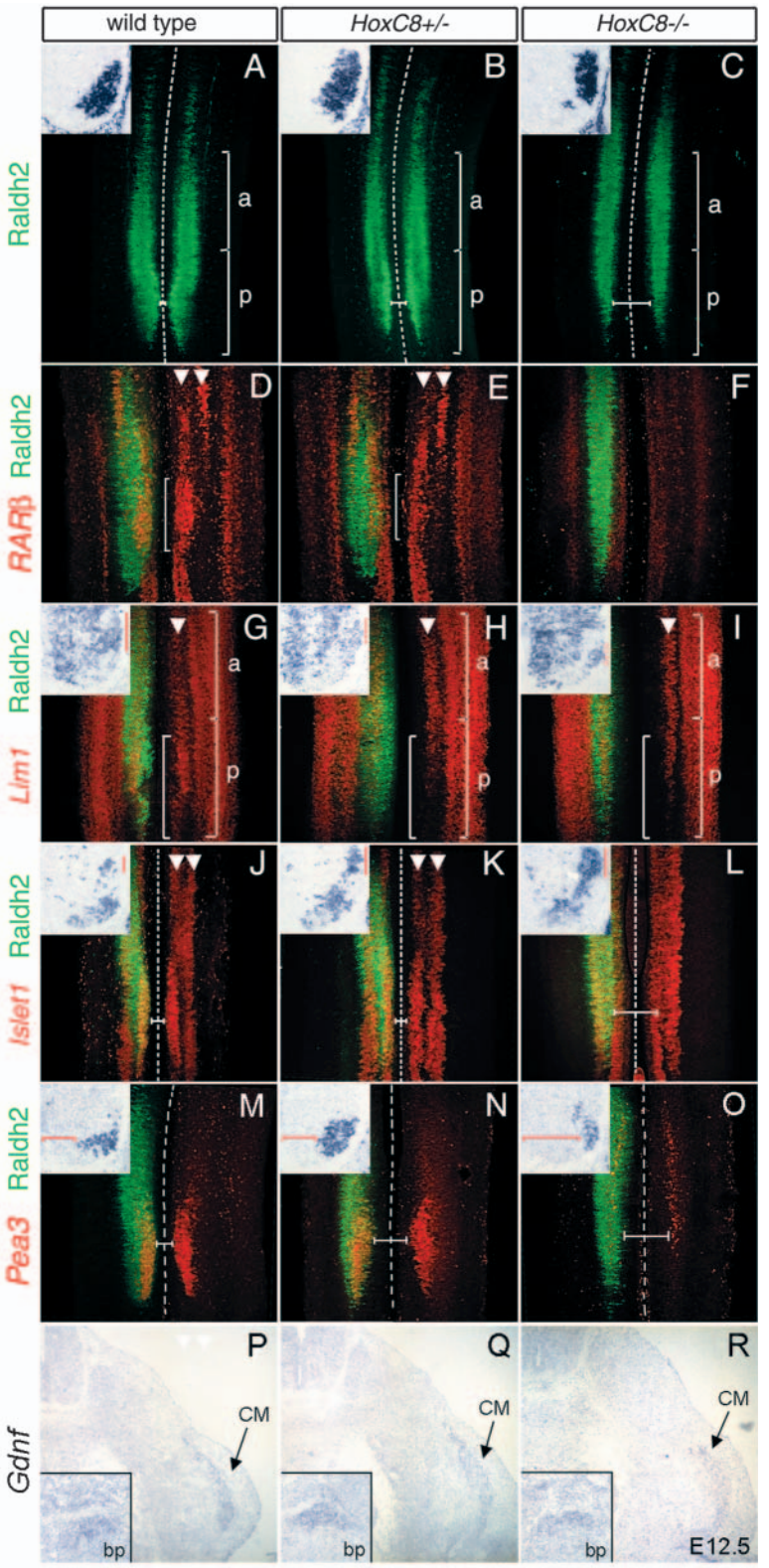

Fig. 8. Loss of Hoxc8 function phenocopies the molecular defects observed in *Raldh2*$^{L-/-}$ spinal cord. Expression of Raldh2 protein (A-C) and selected molecular markers (D-O) on E12.5 flat-mounted spinal cords at brachial level. All the insets represent in-situ hybridization of transverse sections at the middle posterior LMC level (level of the horizontal bars in J-O). (C) In the *Hoxc8*$^{-/-}$ posterior LMC region, the distance between the ventral midline (dotted line) and the Raldh2+ cells is increased (compare horizontal bars in A and C). (D-O) Composite images in which Raldh2 protein is shown on the left side only. (D-F) Decreased *RAR*β expression in the posterior medial LMC domain in the *Hoxc8*$^{+/-}$ spinal cord (brackets, D,E). (F) In *Hoxc8*$^{-/-}$ mutant, *RAR*β expression is absent throughout the LMC. (G-I) *Lim1* expression is diminished in the posterior LMC of *Hoxc8*$^{+/-}$ and *Hoxc8*$^{-/-}$ mutants (brackets). (J-L) The outline of the two *Islet1*+ motor columns is marked by arrowheads. (L) No segregation of motoneurons into columns is visible in *Hoxc8*$^{-/-}$ spinal cord. (M-O) Horizontal bars (white, red in insets) delineate the bigger distance between the ventral midline (dotted line) and the *Pea3*+ cells in *Hoxc8*$^{+/-}$ and *Hoxc8*$^{-/-}$ mutants compared with wild type. (O) In *Hoxc8*$^{-/-}$ mutant, *Pea3* expression is greatly reduced throughout the LMC. (P-R) *Gdnf* transcripts on transverse sections at thoracic level and brachial plexus level (bp; insets). a, anterior; CM, cutaneous maximus; p, posterior.

motoneurons and the migration of these cells are both regulated by Gdnf, this trophic factor is unlikely to be responsible for the migratory defect observed in the *Raldh2*$^{L-/-}$ mutants (Fig. 5I-L). Indeed, we did not detect any change in the distribution and level of *Gdnf* transcripts in mutants. This result contrasts with the marked decrease in RA activity at the level of the brachial plexus and the hypaxial LD and CM muscles, i.e. at the same sites as *Gdnf* expression, in *Raldh2*$^{L-/-}$ mutants (Fig. 5). Possible explanations are that RA activity does not regulate *Gdnf* in the tissues, or that the remaining RA activity present in mutants is sufficient to allow normal expression levels of this factor. In any event, these data strengthen the idea that most of the molecular defects described in *Raldh2*$^{L-/-}$ mutants are linked to an RA deficiency within the LMC.

The mispositioning of Pea3+ cells, which are constituted by over 95% of Islet1+ cells at segmental levels C7/8 (Livet et al., 2002), is very probably a consequence of the redistribution of Islet1+ cells within the *Raldh2*$^{L-/-}$ LMC, as observed at E12.5 (Fig. 4). The early loss or the incomplete specification of some Lim1+ cells and the change in the expression patterns of *Epha4*, cadherins 8 and 7 (Fig. 5), which encode for adhesion molecules regulating motor pool segregation (Price et al., 2002; Coonan et al., 2003), may be responsible for the mispositioning of *Islet1*+ cells. It is noteworthy that the positioning of motor cell bodies can influence peripheral axonal projections, as it has been demonstrated by single cell transplantation experiments in zebrafish embryos or by retrograde labeling in *Hoxc8* mutant mice (Eisen, 1991; Tiret et al., 1998). The alteration of Islet1+ cell distribution in *Raldh2*$^{L-/-}$ mutants could, therefore, lead to subtle aberrant axonal projections.

Lateral LMC specification requires RA signaling and Hox gene function

We found that the loss of Raldh2 function in the lateral LMC was dispensable for the specification of a large subset of lateral LMC cells, as shown by the relatively subtle alterations of

Lim1 expression in the developing spinal cord and the subsequent correct innervation of most dorsal limb muscles in *Raldh2*$^{L-/-}$ mutants. Although the present conditional knockout does not completely rule out a contribution of RA produced by paraxial mesoderm or meningeal cells in the process of lateral LMC specification, our data show that RA was not the only signal to specify this cell fate. Strikingly, the molecular features of the *Raldh2*$^{L-/-}$ mutants, such as the loss of *Lim1*+ motoneurons, the redistribution of *Islet1*+ cells or the downregulation of *Rarb* in the posterior medial LMC, were shared with *Hoxc8* mutants (Fig. 8). We thus demonstrated that Hoxc8 is a key molecule, together with RA signaling, in directing a lateral LMC fate. This finding, along with work on the function of Hoxc6 and Hoxc9 in the specification of a brachial or thoracic motoneuron fate (Dasen et al., 2003), unveils novel roles for Hox proteins within postmitotic differentiating neurons.

The closest phenocopy of the *Raldh2*$^{L-/-}$ phenotype was found in *Hoxc8*$^{+/-}$ heterozygous mutants, indicating that a decrease in the level of Hoxc8 protein is sufficient to modify the specification of a lateral LMC cell type. This finding underlines the importance of the regulation of *Hoxc8* gene expression in postmitotic cells of the ventral spinal cord. At the protein level, Hoxc8 activity is regulated by the presence of co-factors such as the Meis proteins (Popperl et al., 1995). Interestingly, we found that Meis2 was expressed in the *Lim1*+ posterior LMC, and was excluded from the *Islet1*+ posterior domain (J.V. and I.L.R., unpublished), suggesting that Hoxc8 and Meis2 co-expression spatially restricts Hoxc8 function to the lateral LMC. *Hoxc8*$^{-/-}$ mutants clearly display more drastic brachial spinal cord abnormalities than *Raldh2*$^{L-/-}$ mutants. This may reflect an absolute requirement for Hoxc8 in the regulation of some target genes and/or an early requirement for Hoxc8 in neural progenitors or paraxial mesoderm, which would set up the anterior boundary of the LMC.

In conclusion, our results provide new insights into the specification of LMC cell fates. Raldh2 expressed in the LMC provides local RA activity that is transduced by RARβ and activates the expression of the lateral LMC marker Lim1 and allows a correct positioning of cell bodies within the LMC. A recent study demonstrated a bi-directional regulation between Hox genes (*Hoxb4* and *Hoxd4*) and RARβ during the formation of rhombomere boundaries, and showed that the regulatory sequences of each gene contain both active RAREs and Hox consensus binding sites (Serpente et al., 2005). Our results suggest that a similar bi-directional regulation between Hoxc8 and RARβ occurs during the specification and early differentiation of the LMC cells.

We thank V. Fraulob and D. Lagorce for technical help and S. Falcone for animal care. We are indebted to J. Rossant and M. Cappecchi for providing the RARE-*hsplacZ* and RARβCre transgenic mice, respectively. We thank C. Kress for providing the embryonic stem cells (*Hoxc8*) and M. Petkovich, R. Behringer, C-C. Hui, S. Pfaff, C. Henderson, D. Wilkinson, R. Klein, M. Capecchi, X. Desbiens, M. Kmita, A. Esquela Kerscher, T. Jessell and P. Charnay for the gift of antibodies and/or plasmids. We gratefully acknowledge F. Plewniak for help with statistics, N. Ghyselinck, M. Teletin and the Dollé team for helpful discussions. This work was supported by funds from the CNRS, the INSERM, the Collège de France, the Ministère de la Recherche, the Institut Universitaire de France and the Institut Pasteur, and by fellowships from the Association pour la Recherche sur le Cancer (J.V.) and the Fondation pour la Recherche Médicale (J.V., I.L.R.).

References

Abu-Abed, S., Dollé, P., Metzger, D., Beckett, B., Chambon, P. and Petkovich, M. (2001). The retinoic acid-metabolizing enzyme, CYP26A1, is essential for normal hindbrain patterning, vertebral identity, and development of posterior structures. *Genes Dev*. **15**, 226-240.

Appel, B. and Eisen, J. (2003). Retinoids run rampant: multiple roles during spinal cord and motor neuron development. *Neuron* **40**, 461-464.

Baubet, V., Le Mouellic, H., Campbell, A. K., Lucas-Meunier, E., Fossier, P. and Brûlet, P. (2000). Chimeric green fluorescent protein-aequorin as bioluminescent Ca^{2+} reporters at the single-cell level. *Proc. Natl. Acad. Sci. USA* **97**, 7260-7265.

Becker, N., Gilardi-Hebenstreit, P., Seitanidou, T., Wilkinson, D. and Charnay, P. (1995). Characterisation of the Sek-1 receptor tyrosine kinase. *FEBS Lett*. **368**, 353-357.

Berggren, K., McCaffery, P., Drager, U. and Forehand, C. J. (1999). Differential distribution of retinoic acid synthesis in the chicken embryo as determined by immunolocalization of the retinoic acid synthetic enzyme, RALDH-2. *Dev. Biol*. **210**, 288-304.

Carpenter, E. M., Goddard, J. M., Davis, A. P., Nguyen, T. P. and Capecchi, M. R. (1997). Targeted disruption of Hoxd-10 affects mouse hindlimb development. *Development* **124**, 4505-4514.

Chotteau-Lelièvre, A., Dollé, P. and Gofflot, F. (2004). Expression analysis of murine genes using in situ hybridization with radioactive and non-radioactively labeled probes. In *Methods in Molecular Biology: In Situ Hybridization Protocols*, 3rd edn (eds I. A. Darby and T. D. Hewitson). Totowa, NJ: Humana Press (in press).

Colbert, M. C., Rubin, W. W., Linney, E. and LaMantia, A. S. (1995). Retinoid signaling and the generation of regional and cellular diversity in the embryonic mouse spinal cord. *Dev. Dyn*. **204**, 1-12.

Coonan, J. R., Bartlett, P. F. and Galea, M. P. (2003). Role of EphA4 in defining the position of a motor neuron pool within the spinal cord. *J. Comp. Neurol*. **458**, 98-111.

Dasen, J. S., Liu, J. P. and Jessell, T. M. (2003). Motor neuron columnar fate imposed by sequential phases of Hox-c activity. *Nature* **425**, 926-933.

de la Cruz, C. C., Der-Avakian, A., Spyropoulos, D. D., Tieu, D. D. and Carpenter, E. M. (1999). Targeted disruption of Hoxd9 and Hoxd10 alters locomotor behavior, vertebral identity, and peripheral nervous system development. *Dev. Biol*. **216**, 595-610.

de Thé, H., del Mar Vivanco-Ruiz, M., Tiollais, P., Stunnenberg, H. and Dejean, A. (1990). Identification of a retinoic acid-responsive element in the retinoic acid receptor β gene. *Nature* **343**, 177-180.

Diez del Corral, R., Olivera-Martinez, I., Goriely, A., Gale, E., Maden, M. and Storey, K. (2003). Opposing FGF and retinoid pathways control ventral neural pattern, neuronal differentiation, and segmentation during body axis extension. *Neuron* **40**, 65-79.

Eisen, J. S. (1991). Determination of primary motoneuron identity in developing zebrafish embryos. *Science* **252**, 569-572.

Ericson, J., Thor, S., Edlund, T., Jessell, T. M. and Yamada, T. (1992). Early stages of motor neuron differentiation revealed by expression of homeobox gene Islet-1. *Science* **256**, 1555-1560.

Ghyselinck, N. B., Dupé, V., Dierich, A., Messaddeq, N., Garnier, J. M., Rochette-Egly, C., Chambon, P. and Mark, M. (1997). Role of the retinoic acid receptor beta (RARbeta) during mouse development. *Int. J. Dev. Biol*. **41**, 425-447.

Haase, G., Dessaud, E., Garces, A., de Bovis, B., Birling, M., Filippi, P., Schmalbruch, H., Arber, S. and deLapeyrière, O. (2002). GDNF acts through PEA3 to regulate cell body positioning and muscle innervation of specific motor neuron pools. *Neuron* **35**, 893-905.

Helmbacher, F., Schneider-Maunoury, S., Topilko, P., Tiret, L. and Charnay, P. (2000). Targeting of the EphA4 tyrosine kinase receptor affects dorsal/ventral pathfinding of limb motor axons. *Development* **127**, 3313-3324.

Kania, A. and Jessell, T. M. (2003). Topographic motor projections in the limb imposed by LIM homeodomain protein regulation of ephrin-A:EphA interactions. *Neuron* **38**, 581-596.

Kania, A., Johnson, R. L. and Jessell, T. M. (2000). Coordinate roles for LIM homeobox genes in directing the dorsoventral trajectory of motor axons in the vertebrate limb. *Cell* **102**, 161-173.

Landmesser, L. T. (2001). The acquisition of motoneuron subtype identity and motor circuit formation. *Int. J. Dev. Neurosci.* **19**, 175-182.

Le Mouellic, H., Lallemand, Y. and Brûlet, P. (1992). Homeosis in the mouse induced by a null mutation in the Hox-3.1 gene. *Cell* **69**, 251-264.

Liu, J. P., Laufer, E. and Jessell, T. M. (2001). Assigning the positional identity of spinal motor neurons: rostrocaudal patterning of Hox-c expression by FGFs, Gdf11, and retinoids. *Neuron* **32**, 997-1012.

Livet, J., Sigrist, M., Stroebel, S., De Paola, V., Price, S. R., Henderson, C. E., Jessell, T. M. and Arber, S. (2002). ETS gene Pea3 controls the central position and terminal arborization of specific motor neuron pools. *Neuron* **35**, 877-892.

Maina, F., Hilton, M. C., Ponzetto, C., Davies, A. M. and Klein, R. (1997). Met receptor signaling is required for sensory nerve development and HGF promotes axonal growth and survival of sensory neurons. *Genes Dev.* **11**, 3341-3350.

Mathis, L., Kulesa, P. M. and Fraser, S. E. (2001). FGF receptor signalling is required to maintain neural progenitors during Hensen's node progression. *Nat. Cell Biol.* **3**, 559-566.

Mic, F. A., Haselbeck, R. J., Cuenca, A. E. and Duester, G. (2002). Novel retinoic acid generating activities in the neural tube and heart identified by conditional rescue of Raldh2 null mutant mice. *Development* **129**, 2271-2282.

Moon, A. M., Boulet, A. M. and Capecchi, M. R. (2000). Normal limb development in conditional mutants of Fgf4. *Development* **127**, 989-996.

Niederreither, K., McCaffery, P., Dräger, U. C., Chambon, P. and Dollé, P. (1997). Restricted expression and retinoic acid-induced downregulation of the retinaldehyde dehydrogenase type 2 (RALDH-2) gene during mouse development. *Mech. Dev.* **62**, 67-78.

Niederreither, K., Subbarayan, V., Dollé, P. and Chambon, P. (1999). Embryonic retinoic acid synthesis is essential for early mouse post-implantation development. *Nat. Genet.* **21**, 444-448.

Niederreither, K., Vermot, J., Fraulob, V., Chambon, P. and Dollé, P. (2002). Retinaldehyde dehydrogenase 2 (RALDH2)-independent patterns of retinoic acid synthesis in the mouse embryo. *Proc. Natl. Acad. Sci. USA* **99**, 16111-16116.

Novitch, B. G., Wichterle, H., Jessell, T. M. and Sockanathan, S. (2003). A requirement for retinoic acid-mediated transcriptional activation in ventral neural patterning and motor neuron specification. *Neuron* **40**, 81-95.

Popperl, H., Bienz, M., Studer, M., Chan, S. K., Aparicio, S., Brenner, S., Mann, R. S. and Krumlauf, R. (1995). Segmental expression of Hoxb-1 is controlled by a highly conserved autoregulatory loop dependent upon exd/pbx. *Cell* **81**, 1031-1042.

Price, S. R., De Marco Garcia, N. V., Ranscht, B. and Jessell, T. M. (2002). Regulation of motor neuron pool sorting by differential expression of type II cadherins. *Cell* **109**, 205-216.

Rijli, F. M., Matyas, R., Pellegrini, M., Dierich, A., Gruss, P., Dollé, P. and Chambon, P. (1995). Cryptorchidism and homeotic transformations of spinal nerves and vertebrae in Hoxa-10 mutant mice. *Proc. Natl. Acad. Sci. USA* **92**, 8185-8189.

Rossant, J., Zirngibl, R., Cado, D., Shago, M. and Giguère, V. (1991). Expression of a retinoic acid response element-hsplacZ transgene defines specific domains of transcriptional activity during mouse embryogenesis. *Genes Dev.* **5**, 1333-1344.

Sakai, Y., Meno, C., Fujii, H., Nishino, J., Shiratori, H., Saijoh, Y., Rossant, J. and Hamada, H. (2001). The retinoic acid-inactivating enzyme CYP26 is essential for establishing an uneven distribution of retinoic acid along the anterio-posterior axis within the mouse embryo. *Genes Dev.* **15**, 213-225.

Scardigli, R., Baumer, N., Gruss, P., Guillemot, F. and Le Roux, I. (2003). Direct and concentration-dependent regulation of the proneural gene Neurogenin2 by Pax6. *Development* **130**, 3269-3281.

Serpente, P., Tümpel, S., Ghyselinck, N., B., Niederreither, K., Wiedemann, L. M., Dollé, P., Chambon, P., Krumlauf, R. and Gould, A. P. (2005). Direct cross-regulation between RARβ and Hox genes during hindbrain segmentation. *Development* **132**, 503-513.

Sharma, K., Sheng, H. Z., Lettieri, K., Li, H., Karavanov, A., Potter, S., Westphal, H. and Pfaff, S. L. (1998). LIM homeodomain factors Lhx3 and Lhx4 assign subtype identities for motor neurons. *Cell* **95**, 817-828.

Sockanathan, S. and Jessell, T. M. (1998). Motor neuron-derived retinoid signaling specifies the subtype identity of spinal motor neurons. *Cell* **94**, 503-514.

Sockanathan, S., Perlmann, T. and Jessell, T. M. (2003). Retinoid receptor signaling in postmitotic motor neurons regulates rostrocaudal positional identity and axonal projection pattern. *Neuron* **40**, 97-111.

Solomin, L., Johansson, C. B., Zetterstrom, R. H., Bissonnette, R. P., Heyman, R. A., Olson, L., Lendahl, U., Frisen, J. and Perlmann, T. (1998). Retinoid-X receptor signalling in the developing spinal cord. *Nature* **395**, 398-402.

Sucov, H. M., Murakame, K. K. and Evans, R. M. (1990). Characterisation of an autoregulated response element in the mouse retinoic acid receptor β gene. *Proc. Natl. Acad. Sci. USA* **87**, 5392-5396.

Thaler, J. P., Koo, S. J., Kania, A., Lettieri, K., Andrews, S., Cox, C., Jessell, T. M. and Pfaff, S. L. (2004). A postmitotic role for Isl-class LIM homeodomain proteins in the assignment of visceral spinal motor neuron identity. *Neuron* **41**, 337-350.

Tiret, L., Le Mouellic, H., Maury, M. and Brûlet, P. (1998). Increased apoptosis of motoneurons and altered somatotopic maps in the brachial spinal cord of Hoxc-8-deficient mice. *Development* **125**, 279-291.

Tosney, K. W., Hotary, K. B. and Lance-Jones, C. (1995). Specifying the target identity of motoneurons. *BioEssays* **17**, 379-382.

Tsuchida, T., Ensini, M., Morton, S. B., Baldassare, M., Edlund, T., Jessell, T. M. and Pfaff, S. L. (1994). Topographic organization of embryonic motor neurons defined by expression of LIM homeobox genes. *Cell* **79**, 957-970.

Vermot, J., Niederreither, K., Garnier, J. M., Chambon, P. and Dollé, P. (2003). Decreased embryonic retinoic acid synthesis results in a DiGeorge syndrome phenotype in newborn mice. *Proc. Natl. Acad. Sci. USA* **100**, 1763-1768.

Vooijs, M., Jonkers, J. and Berns, A. (2001). A highly efficient ligand-regulated Cre recombinase mouse line shows that LoxP recombination is position dependent. *EMBO Reports* **2**, 292-297.

Zhao, D., McCaffery, P., Ivins, K. J., Neve, R. L., Hogan, P., Chin, W. W. and Dräger, U. C. (1996). Molecular identification of a major retinoic-acid-synthesizing enzyme, a retinaldehyde-specific dehydrogenase. *Eur. J. Biochem.* **240**, 15-22.